Elastic Scattering of Fast Neutrons by He^4†

JOHN D. SEAGRAVE
Los Alamos Scientific Laboratory, University of California, Los Alamos, New Mexico
(Received August 24, 1953)

Angular distributions of neutrons scattered by helium have been measured at five neutron energies between 2.6 and 14 Mev. A large proportional counter filled with helium and krypton was employed, and the distribution in energy of alpha particles recoiling from collimated neutrons observed. All five distributions are similar, and are characterized by strong scattering of the neutrons in the forward direction, a minimum for neutrons scattered near 120° in the center-of-mass system, and a smaller peak for back-scattering. The location of the minimum moves forward and the ratio of differential cross sections $\sigma_{\mathrm{back}}/\sigma_{\mathrm{min}}$ increases smoothly with increasing neutron energy over the range studied. The observed angular distributions are in good agreement with the distributions predicted from analysis of p-He^4 scattering, and support the large splitting of the P states of He^5, and the very broad width of the $P_{\frac{1}{2}}$ state. A summary of n-He^4 phase shifts and recent total cross-section measurements is given.

I. INTRODUCTION

A. Previous Work

THE angular distribution of fast neutrons scattered by He^4 has been studied in the neutron energy region 0.4 to 2.73 Mev by Adair,[1] using a proportional counter, and the region has recently been extended to 4.15 Mev by Huber and Baldinger,[2] using a parallel-plate ionization chamber. Two cloud-chamber investigations at very high neutron energies have been reported,[3,4] but the results are inconclusive for neutron energies less than 40 Mev. Dodder and Gammel[5] have analyzed existing data for p-He^4 elastic scattering up to $E_p=9.5$ Mev in terms of nuclear reaction theory[6–9] and have applied their results for Li^5 to the description of the mirror nucleus He^5 and n-He^4 scattering. Their analysis accounts more successfully for the variation with energy of the n-He^4 total cross section[10] than does that of Adair[1] but leads to phase shifts in disagreement with those derived from the angular distributions observed[2] in the region $E_n=3$ to 4 Mev, particularly with respect to the broad $P_{\frac{1}{2}}$ state of He^5. However, extrapolation of the theoretical analysis to a neutron energy of 14.1 Mev, together with certain assumptions about the d-wave phase shifts, leads to prediction of a total cross section of 1.04 barns, which compares well with the experimental value of 1.03 ± 0.02 barns.[11]

B. Scope and Method of Present Investigation

The work reported below was undertaken initially as part of the program of study of interactions of 14-Mev neutrons with nuclei carried on by this laboratory, with the object of obtaining the angular distribution of n-He^4 scattering at $E_n=14$ Mev and comparing it with theory,[5] in hope of obtaining more information about the d-wave interactions. It was, in addition, possible to make measurements at 2.6, 4.5, 5.5, and 6.5 Mev, where certain of the difficulties encountered in the 14-Mev measurements were less troublesome.

Neutrons scattered elastically from light nuclei lose an appreciable part of their energy to the recoiling nucleus. In the case of 14-Mev neutrons on He^4, the scattered neutrons range in energy from 14 to 5 Mev, and direct observation of the scattered neutrons is impracticable. A much more satisfactory method in such a case is to observe the recoiling charged particles, since the angular distribution of the neutron in the center-of-mass system is directly proportional to the energy distribution of the recoiling target nucleus in the laboratory system.[12] This relation can be put into the form $4\pi\sigma(\cos\theta_n)=\sigma_T E_{\mathrm{max}}P(E)$, where $\sigma(\cos\theta_n)=d\sigma/d\Omega$ is the differential elastic-scattering cross section at the cm neutron angle θ_n, σ_T is the total (elastic) cross section, and $P(E)$ is the recoil energy distribution function (number per unit energy interval). This method has been used to study neutron scattering by hydrogen, deuterium, helium, carbon (CS_2), and oxygen[1,2,12–16] for neutron energies up to 4 Mev.

II. EXPERIMENTAL TECHNIQUE

A. Choice of Counter

In their investigation of n-He^4 scattering to $E_n=4.14$ Mev, Huber and Baldinger[2] employed a parallel-plate ionization chamber. Sixteen atmospheres of helium were required to reduce the range of the most energetic recoils to 7 mm. An extension of their technique to $E_n=14$ Mev would require over 100 atmospheres of

† Work performed under the auspices of the U. S. Atomic Energy Commission.
1 R. K. Adair, Phys. Rev. **86**, 155 (1952).
2 P. Huber and E. Baldinger, Helv. Phys. Acta **25**, 435 (1952).
3 C. Schwartz, Phys. Rev. **85**, 73 (1952).
4 P. Tannenwald, Phys. Rev. **89**, 508 (1953).
5 D. C. Dodder and J. L. Gammel, Phys. Rev. **88**, 520 (1952).
6 C. L. Critchfield and D. C. Dodder, Phys. Rev. **76**, 602 (1949).
7 E. P. Wigner and L. Eisenbud, Phys. Rev. **72**, 29 (1947).
8 Feshbach, Peaslee, and Weisskopf, Phys. Rev. **71**, 145 (1947).
9 R. G. Thomas, Phys. Rev. **80**, 136 (1950).
10 Bashkin, Mooring, and Petree, Phys. Rev. **82**, 562 (1951).
11 Coon, Graves, and Barschall, Phys. Rev. **88**, 562 (1952); and J. H. Coon (private communication).
12 H. H. Barschall and M. H. Kanner, Phys. Rev. **58**, 590 (1940).
13 J. H. Coon and H. H. Barschall, Phys. Rev. **70**, 592 (1946).
14 T. A. Hall and P. G. Koontz, Phys. Rev. **72**, 196 (1947).
15 Baldinger, Huber, and Proctor, Phys. Rev. **84**, 1058 (1951).
16 Huber, Baldinger, and Budde, Helv. Phys. Acta **25**, 444 (1952).

helium to give a similar range of recoil and introduce formidable mechanical and electrical problems. The addition of another "stopping" gas is clearly required for an extension to higher energies.

Adair[1] employed a proportional counter similar to that of Hall and Koontz[14] except for the addition of guard sleeves held at an intermediate potential.[17]

The counter employed in the present investigation was made from 3-in. o.d. by $\frac{1}{16}$-in. wall brass tube, about 14 in. long, with an active length limited to 6 in. by hypodermic needles in a manner described previously.[18,19] The counter wall was lined with platinum and the central wire was 0.005-in. Pt wire. The counter was modified so that an alpha-active deposit of Pu^{239} could be exposed through a hole in the wall, or removed at will. Subsequently, a Pu^{239} deposit was added on the center wire. Operation of the counter could be checked frequently with the aid of these sources, and they provided a reference pulse height (5.16 Mev).

Nearly all materials are disintegrated to some extent by 14-Mev neutrons.[20] However, Pt and Au liners are effective in reducing background pulses from counter walls. Krypton was chosen as the "stopping" gas on the basis of a comparison[21] of A, Kr, and Xe. Kr and Xe give less than $\frac{1}{10}$ as much "gas background" in the region of interest as does A, and moreover the Kr pulse-height spectrum exhibits a minimum near the 9-Mev end point of the He recoil spectrum.

Provision was made for continuous purification of the filling gases by convective circulation over hot calcium metal turnings.[22]

B. Collimators

The strength of the neutron sources available permitted the "luxury" of a collimator of neutrons to localize and render calculable the wall effect. All data were taken with the collimated neutron "beam" transverse to the counter axis and symmetrically located on the sensitive volume. Two collimators made of steel were used: (a) a cylinder 46 cm long, with 1-in. inside diameter and (b) a hollow pyramid 10.5 in. long of angular aperture approximately 9 by 14 degrees. Type (a) was used at $E_n=14.3$ Mev and Type (b) at the lower energies where the mean free path of neutrons in iron is smaller, and the larger solid angle was desired to compensate for the smaller source strengths available.

C. Wall Effects

A correction to the observed pulse-height distributions for recoils which collide with the wall can be made under certain simplifying assumptions: (a) Geiger's formula for alpha-particle ranges $R\sim v^3\sim E^{1.5}$ holds;[23] (b) entrance wall effects can be neglected, due to the effect of collimation and the low-energy limit of usable data (see below); (c) local curvature of the exit wall can be neglected, so that the maximum distance from which a recoil of given energy (or angle) can strike the wall can be averaged over azimuthal angles by taking the projection of its range along the direction of the incident neutron. The "collision distance" so defined can then be expressed as $D(E)=R_0(E/E_0)^2$ by using assumptions (a) and (c) and the relation $E=E_0\cos^2\theta$, where R_0 is the range corresponding to the maximum recoil energy E_0. Calculation of the fraction affected of recoils of energy E can be reduced to calculation of the volume a collision distance $D(E)$ deep from the (curved) wall. The distribution of the degraded pulses can be calculated from the range-energy relation. Errors involved in the above assumptions are small compared to the magnitude of the final correction term. Details will not be given for the calculations of geometrical factors and distribution functions, but the procedure was as follows. Let the recoil energy distribution function be expanded in the form $P(E)=\sum A_nE^n$. The distorted pulse-height distribution function can be developed in the form $p(\xi)=\sum A_nF_n(\xi,\alpha)$, where α is the ratio of maximum recoil range to counter diameter, ξ is the pulse height, and the functions F_n are calculated as outlined above for the geometries in use. Since the coefficients A_n are unknown, they were obtained from the data by an iterative procedure. The observed pulse-height distributions were represented by a power series using the method of least squares. The preliminary coefficients so determined were employed in the above formalism to determine preliminary corrections, which were subtracted from the data. The resulting "corrected" data were re-analyzed and the procedure repeated as a check. However, since the maximum correction applied to any point was 15 percent for some of the data at 14 Mev, and less than 7 percent for the lower-energy data, this procedure converged rapidly, and the second fit was not significantly different from the first.

D. Electronics and Counter Operation

The electronic equipment included a Los Alamos Model 101 amplifier and preamplifier, found to be linear (within 1 percent) for output voltages to 165 volts. This amplifier was usually used with an RC pulse-clipping time of 32 microseconds. A battery box was used for counter voltage and its output monitored. The amplified pulses were displayed on an 18-channel pulse-height analyzer,[24] which greatly facilitated taking data rapidly and reliably.

[17] A. L. Cockroft and S. C. Curran, Rev. Sci. Instr. **22**, 37 (1951).

[18] J. H. Coon and R. A. Nobles, Rev. Sci. Instr. **18**, 44 (1947).

[19] A description of the prototype counter together with its operation at high pressures is given in Los Alamos Report LA-1135, by John Wahl (unpublished).

[20] E. B. Paul and R. L. Clarke, Can. J. Phys. **31**, 267 (1953).

[21] F. L. Ribe, private communication (to be published).

[22] W. Jentschke and S. Prankl, Physik. Z. **40**, 706 (1939).

[23] The relation $R\sim E$ was used for $E_n=2.61$ Mev and the correction carried out as outlined for $R\sim E^{1.5}$.

[24] C. W. Johnstone, Nucleonics **11**, No. 1, 36 (1953).

Although krypton made a fairly satisfactory high-pressure counter filling, counter performance was markedly affected by the presence of helium. Resolution of the Pu^{239} alphas deteriorated steadily with increasing partial pressure of helium, yet the original resolution of about 5 percent was restored when the krypton was condensed in the counter and the helium pumped off. Study of the resolution as a function of purification time of the gas circulating over calcium metal at 300°C showed very little improvement. To explore this effect the counter was provided with a deposit of Pu^{239} on the center wire in addition to the removable wall deposit, so that the behavior of the counter with respect to both central and wall pulses could be studied for a variety of operating conditions. Extensive efforts were made to improve the purity of the gas fillings, and progress was followed by frequent analyses with a mass spectrometer, while the counter operation was followed as outlined above. No consistent improvement resulted. For a given filling, the general behavior of the alpha pulses as a function of gas multiplication was as follows.

At unit gas multiplication, the wall-to-center pulse-height ratio was about 1.3, and the resolution of each group was poor. As multiplication was increased, the ratio decreased and the resolution improved until an optimum resolution was obtained in the vicinity of a multiplication of 8. For higher multiplication, although the wall-to-center ratio approached unity, the resolution deteriorated rapidly. The resolution of the He-recoil end point was also observed for several conditions, and it was found that best resolution of the end point corresponded to the above "optimum" operating conditions. The wall-to-center pulse-height ratio was about 1.1, but the apparent end point of the recoils fell at a point consistent with taking the mean Pu^{239} alpha pulse height as an energy calibration. The operation of the counter was optimized in the manner described for all the data reported below.

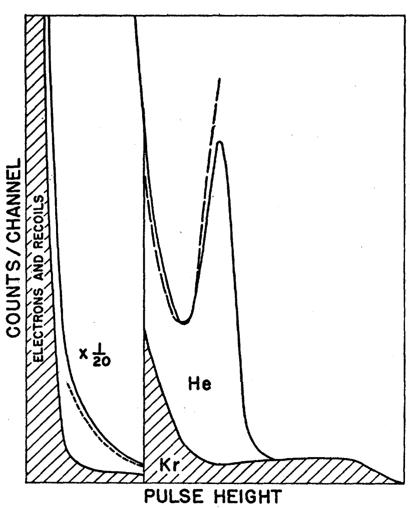

FIG. 1. Composite pulse-height distribution for a typical set of data at $E_n=14.3$ Mev. Solid curve is observed distribution, shaded region is gas background included, and dotted curve represents the modification of the net helium distribution by the wall-effect correction. Counter filling was 75-psi krypton+15-psi helium.

E. Background and Limitations of the Method

Krypton was chosen as the stopping gas for its low "gas background" at $E_n=14$ Mev, but the Kr/He counting ratio was not negligible, being about one-third in the worst case. Better counter operation could be obtained with a larger Kr/He pressure ratio, but at the expense of larger relative background. The addition of CO_2 to the counter filling reduced the pulse rise time, but did not improve the resolution materially, and contributed to the gas background. Use of CO_2 was abandoned. The following procedure was adopted to measure the gas background. After a He+Kr run, one end of the counter was immersed in a bowl of liquid nitrogen to condense the krypton and the helium pumped off until an indicated pressure of 1 mm was reached. The counter was then sealed off and prepared for bombardment. As soon as the counter had warmed to room temperature, the operating conditions were made as nearly as possible like those under which the first run was made. Krypton pressure and collimator geometry being the same in both cases, the principle uncertainty in the "background" spectrum was in the pulse-height energy scale. Fortunately, the krypton reaction spectrum extends to 16 Mev, while the helium recoil spectrum ends at 9 Mev, so the excess could be used as an additional check on the energy scale.

One of the limitations of this method of measuring the angular distribution is that it does not give information (directly) about neutrons scattered through small angles, since the pulses from the corresponding low-energy recoils are masked by pulses due to electrons and recoils from heavier nuclei. Because of the high pressures of krypton required, the gamma or electron end point was about 2 Mev for $E_n=14$ Mev, which corresponds to a neutron scattering angle of 57°. The krypton recoil end point was only 0.75 Mev. In the results to be presented, the data lying in the electron-masked region are not included because of the large statistical uncertainty of "net" data obtained by subtracting large numbers, although the results are consistent with the indicated extrapolations from the reliable data.

Information about backscattered neutrons is limited by the finite resolution of the counter, since the cusp at the end point of the energy distribution function is smeared out in the corresponding pulse-height distribution. No correction was made for the effect of finite resolution on the basis of the following calculation. The preliminary least-squares fit to the central portion of the data was smeared numerically by a resolution function of the same form as the distribution function observed for the wall-alphas, and only the data which were substantially unaffected by the operation were retained for correction for the wall-effect.

The nature and extent of these corrections and limitations can be better appreciated by comparison of Figs. 1 and 2, which show a composite of the raw data and the final results, respectively, for $E_n = 14.3$ Mev. Figure 1 is included only to give a general perspective, so the actual data points are not shown, but the relation of observed distributions, the electron "stone wall," and the effects of finite resolution and finite range of the recoils may be seen.

III. EXPERIMENTAL RESULTS

A. $E_n = 14.3 \pm 0.1$ Mev

These measurements were made at the 250-kev Cockcroft-Walton accelerator, using the D-T reaction in a thick Zr-T target. Counter fillings were in the neighborhood of 80-psi krypton and 20-psi helium.

In Fig. 2 are shown the results of three independent measurements of the angular distribution of 14.3-Mev neutrons scattered by He^4. The solid curve is the distribution predicted by the theory of Dodder and Gammel.[5] Since the three runs were consistent with each other and with the theory for the backscattering hemisphere within the statistical uncertainty, no distinction between runs was made in plotting the composite results. However, for the usable portion of the data in the forward hemisphere, the three runs differ significantly and are distinguished by dotted lines. It is believed that these departures represent the effect of inelastic neutrons produced in the target assembly and in the steel collimator. Lower-energy neutrons can be especially troublesome because the n-He^4 cross section is larger (roughly as $E^{-\frac{1}{2}}$), and they will produce more pulses per unit energy interval (as E^{-1}). Present information on the cross section and spectrum of 14-Mev neutrons inelastically scattered by iron[25] is consistent with this interpretation, but it was not feasible to calculate a correction for the effect of such neutrons on the pulse-height distribution. If this interpretation is correct, the differing flux of inelastic neutrons reflects small differences in the collimator geometry of the three independent runs. As a test of the theory, however, the shape of the curve for backscattering is much more sensitive to small changes in phase shifts than is the shape in the other hemisphere, and the agreement is quite good, considering the experimental difficulties and the uncertainties in the theory.[26] The data do not warrant analysis for phase shifts. It should be understood that the *absolute* cross section scale was not determined in this experiment; the data were normalized to independent total cross-section measurements.

[25] E. R. Graves and L. Rosen, Phys. Rev. **89**, 343 (1953); Louis Rosen (private communication).

[26] Since this work was completed, an angular distribution over all angles at $E_n = 14.1$ Mev has been obtained by cloud-chamber techniques at the Rice Institute [J. R. Smith (private communication)], and it is also in good agreement with the theory.

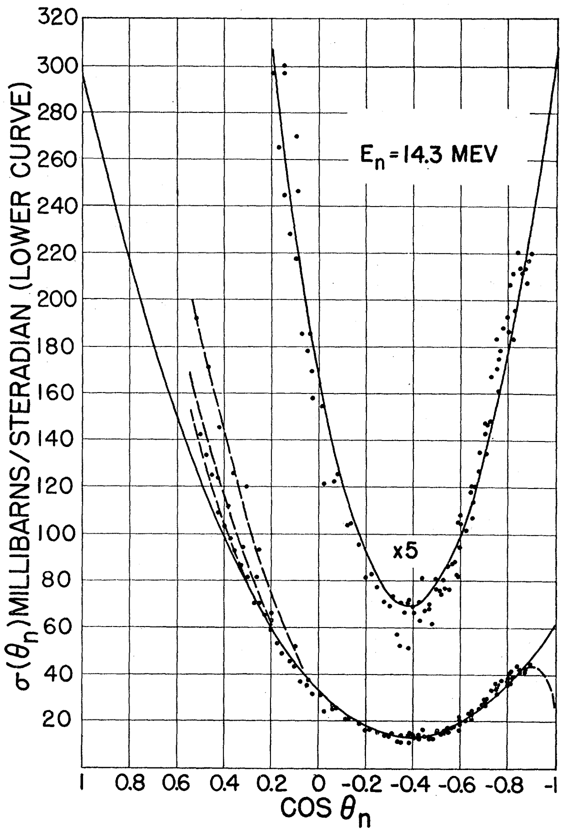

FIG. 2. Comparison of experimental and theoretical results for angular distribution of 14.3-Mev neutrons scattered by helium. θ_n is the angle through which the neutron is scattered in the center-of-mass system. Experimental points for three independent observations are distinguished by dotted curves. The disparities observed are attributed to the effects of energy-degraded neutrons present in the incident flux.

B. $E_n = 4.53 \pm 0.06$, 5.54 ± 0.06, and 6.50 ± 0.06 Mev

These measurements were made at the large Los Alamos Van de Graaff, using the D−D reaction in a gas target, and the short pyramidal collimator. The three lower curves in Fig. 3 show the distributions obtained at these three neutron energies. Although it is possible that at these lower energies, a He−A−CO_2 filling would have given satisfactory results, the measurements were carried out with a He+Kr filling similar to that used at $E_n = 14.3$ Mev, to test whether any systematic error could be attributed to counter operation with this filling or to the wall-effect correction, the latter being less than half as large a correction in this region. No evidence for such effects was found. Performance of the collimator at these energies was checked with a Np^{237} spiral fission chamber and with a stilbene scintillator. The collimator was found to produce about 10 percent scattering-in on the axis, but this increase in flux was due almost exclusively to elastic scattering from iron, which would have no detectable effect on the neutron or recoil spectra.

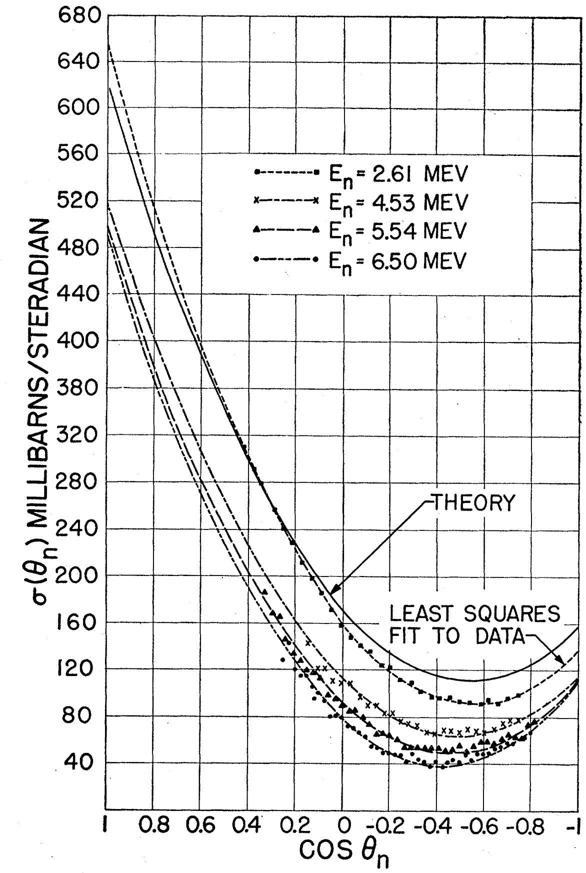

FIG. 3. Comparison of theoretical curves and experimental data for $E_n=6.50$, 5.54, 4.53, and 2.61 Mev. A separate "experimental" curve is shown only for $E_n=2.61$ Mev.

Because of the high pressure of krypton, the electron end point was about 1.5 Mev, which prevented obtaining usable data below about 1 Mev for the helium recoils. The available neutron intensity made the data less reliable statistically than those at 14.3 Mev, but the results seem to be in satisfactory agreement with the theoretical prediction. Only theoretical curves are given in Fig. 2 for these three energies, as no separate "experimental" curve seems warranted.

C. $E_n=2.61\pm0.06$ Mev

This measurement was made at the Cockcroft-Walton accelerator, using a collimated neutron "beam" at 75 degrees from the bombarding deuteron beam. In this case neutrons were obtained from the D−D reaction, and the short collimator was used. The counter filling was 15-psi krypton and 15-psi helium. The data are also shown in Fig. 3. The experimental curve appears to depart significantly from the theoretical prediction. A parabola can be fitted to the corrected data with quite small mean square deviation, the fit being better than 2 percent at any point. This curve was used in an attempt to analyze for phase shifts which would be in better agreement with the experiment.

IV. COMPARISON WITH THEORY

A. Phase Shift Analysis

For neutrons scattered elastically by nuclei for which $J=0$, the differential cross section is given by[27]

$$k^2\sigma(\mu)=\left|\sum\{(l+1)\sin\delta_l^+\exp(i\delta_l^+)+l\sin\delta_l^-\exp(i\delta_l^-)\}P_l(\mu)\right|^2+(1-\mu^2)\left|\sum\{\sin\delta_l^+\exp(i\delta_l^+)-\sin\delta_l^-\exp(i\delta_l^-)\}P_l'(\mu)\right|^2, \quad (1)$$

where k is the neutron wave number, and $\mu=\cos\theta$. We are concerned with $l\leq 2$, and with $S_{\frac12}$, $P_{\frac12}$, $P_{\frac32}$, $D_{\frac32}$, and $D_{\frac52}$ phase shifts, designated δ_0, δ_1^-, δ_1^+, δ_2^-, and δ_2^+, respectively. Also,

$$k^2\sigma_T=4\pi\sum\{(l+1)\sin^2\delta_l^++l\sin^2\delta_l^-\}. \quad (2)$$

For the graphical interpretation of the shape of elastic scattering resonances,[28] it is convenient to regard $\sin\delta\exp(i\delta)$ as a vector intersecting a unit circle which makes an angle δ with the real axis. In passing through a resonance, the "resonant" vector will trace out its circle, while the others remain nearly constant. For the interpretation of the *angular* variation at fixed energy, it is more convenient to substitute $\sin\delta\exp(i\delta)=\{\exp(2i\delta)-1\}/2i$ in Eq. (1). When a sum of these complex numbers is squared, the factor $|1/2i|^2=\frac14$, and we may rewrite Eq. (1) as

$$4k^2\sigma(\mu)=(1-\mu^2)|\mathbf{P}_{\frac32}-\mathbf{P}_{\frac12}+(\mathbf{D}_{\frac52}-\mathbf{D}_{\frac32})3\mu|^2+|\mathbf{S}_{\frac12}-1+(2\mathbf{P}_{\frac32}+\mathbf{P}_{\frac12}-3)\mu+(3\mathbf{D}_{\frac52}+2\mathbf{D}_{\frac32}-5)\tfrac12(3\mu^2-1)|^2. \quad (3)$$

The bold face symbols are complex vectors *of unit length* which make an angle 2δ with the real axis, where δ is the corresponding phase shift. In a similar manner Eq. (2) may be rewritten

$$k^2\sigma_T=2\pi\{9-\mathrm{Re}(\mathbf{S}_{\frac12}+\mathbf{P}_{\frac12}+2\mathbf{P}_{\frac32}+3\mathbf{D}_{\frac52})\}. \quad (4)$$

A graphical analysis of these relations was carried out for each energy at which a measurement was made, with the result that a "best fit" to the observed distributions did not lead to phase shifts significantly different from those of the theory, except at $E_n=2.61$ Mev. At this energy the d-wave phase shifts are expected to be nearly zero, so Eqs. (3) and (4) can be simplified by setting $\mathbf{D}_{\frac32}=\mathbf{D}_{\frac52}=\mathbf{1}$. Since there remain only three phase shifts, they may be determined from three experimental cross sections, which are most conveniently taken to be σ_T, $\sigma(1)$, and $\sigma(-1)$. From Eq. (3),

$$4k^2\sigma(\pm1)=|\mathbf{S}_{\frac12}-\mathbf{1}\pm(2\mathbf{P}_{\frac32}+\mathbf{P}_{\frac12}-\mathbf{3})|^2, \quad (5)$$

in this case. The total cross section can be determined only to within about 20 percent from the incomplete

[27] F. Bloch, Phys. Rev. 58, 829 (1940).
[28] R. A. Laubenstein and M. J. W. Laubenstein, Phys. Rev. 84, 18 (1951).

angular distribution, so the differential cross sections must be normalized by an independent value of the total cross section. Recent measurements at this laboratory[29] of σ_T in the vicinity of 2.61 Mev are 3.16±0.06 barns at 2.49±0.05 Mev and 2.79±0.06 barns at 2.99±0.04 Mev. Taking into account the shape of the σ_T *vs* E_n curve, we may estimate $\sigma_T=3.04\pm0.08$ barns at 2.61 Mev. The resulting uncertainty in normalization dominates the net uncertainty in the angular distributions, or in the values of $\sigma(1)$ and $\sigma(-1)$ calculated from the coefficients of the power-series least-squares fit.

The construction shown in Fig. 4 represents Eqs. (4) and (5). The terminus of the vector sum $\mathbf{S}_{\frac{1}{2}}-\mathbf{1}+(-\mathbf{3}+2\mathbf{P}_{\frac{3}{2}}+\mathbf{P}_{\frac{1}{2}})$ must lie at a distance $2k\sqrt{\sigma}(1)$ from the origin and its real part be $-k^2\sigma_T/2\pi$. These loci, together with the probable error of experimental determination are indicated in the figure and determine an area locus for the vector. Also, according to Eq. (5), the reflection of the **P** vector $-\mathbf{3}+2\mathbf{P}_{\frac{3}{2}}+\mathbf{P}_{\frac{1}{2}}$ through the end point of the **S** vector must fall in the domain determined by $2k\sqrt{\sigma}(-1)$. The locations of the end points $\mathbf{S}\pm\mathbf{P}$ predicted by theory[5] are indicated by solid circles, and it may be seen that they fall slightly outside of the probable error of experimental results. The uncertainty in determination of "experimental" phase shifts and the disagreement with the theory is small (indicated in Fig. 4 by shaded sectors) except for δ_1^-. It can be seen from the diagram how sensitive the "most probable" value of δ_1^- is to the value of the total cross section. For this reason the discrepancy between the present experimental value $\delta_1^-=11\pm6$ degrees and the theoretical estimate $\delta_1^-=20.5$ degree is not very serious. A better determination of the total cross section would be worthwhile, particularly in view of the generally excellent agreement with theory. If the discrepancy is real, it may be interpreted as indicating some curvature in the relation between logarithmic derivative and energy (reference 5, Fig. 1) for the $P_{\frac{1}{2}}$ state (i.e., that

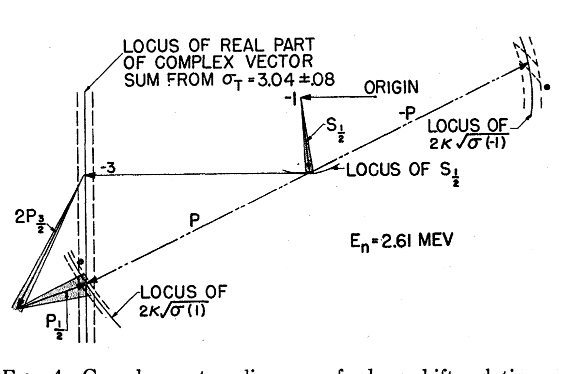

FIG. 4. Complex-vector diagram of phase-shift relations at $E_n=2.61$ Mev. The probable errors of experimental cross sections are indicated by dotted lines, and the corresponding uncertainties in phase shifts are indicated by shaded sectors. The location of the end points of the vectors $\mathbf{S}\pm\mathbf{P}$ predicted by theory are indicated by solid circles (●).

[29] J. H. Coon (private communication).

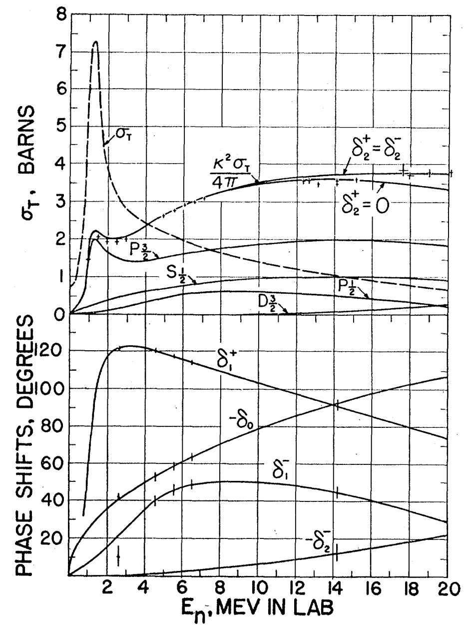

FIG. 5. Summary of phase-shift and cross-section values for the n-He⁴ interaction from $E_n=0$ to 20 Mev. In the lower part of the figure are shown the phase shifts predicted from analysis of the p-He⁴ interaction, together with the values indicated by the present experiment. In the upper part of the figure are shown the total cross section σ_T, the separate terms in the summation of Eq. (2), and their sum $k^2\sigma_T/4\pi$. The results of recent total cross section measurements are plotted in the form $k^2\sigma_T/4\pi$ for two assumptions concerning the $D_{5/2}$ interaction.

the single-level approximation is not quite valid for this broad state).[30]

B. Graphical Summary

Figure 5 is presented as a summary of present information on n-He⁴ scattering up to 20 Mev. In the lower part are shown the phase shifts derived from analysis[5,6] of p-He⁴ scattering, together with the indicated results of the present experiment. At $E_n=2.61$ Mev, the "most probable" values have been plotted together with their probable errors. At the other points, no "most probable" value is given, and the indicated uncertainties were obtained somewhat arbitrarily from the analyses described above, and should be interpreted as the limits outside of which a discrepancy should have been experimentally detectable.

The corresponding cross sections are shown in the upper part of Fig. 5. The curves designated by spectroscopic symbols are the separate terms in Eq. (2), i.e., $(j+\frac{1}{2})\sin^2\delta_l^j$, and the upper curve their sum $k^2\sigma_T/4\pi$. The $D_{\frac{3}{2}}$ phase shifts are those for scattering by a hard sphere of radius 2.9×10^{-13} cm. The $D_{\frac{5}{2}}$ level in He⁵ occurs at an excitation of 16.64 Mev,[31] and should figure

[30] In reference 5, the cm proton energy scales of Fig. 1 and Fig. 2, and the values of E_λ and γ_λ^2 quoted on p. 523 should be multiplied by 1.25. In Eq. (2), the numerator of the first term should read ka/FG.

[31] F. Ajzenberg and T. Lauritsen, Revs. Modern Phys. **24**, 321 (1952). See Fig. 1.

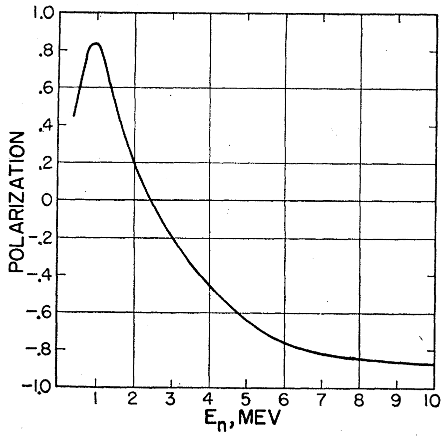

FIG. 6. Polarization of neutrons scattered through 90° in the center-of-mass system.

in neutron scattering at $E_n=22$ Mev, which is well outside the region under consideration. However, very little is known about a possible $D_{\frac{5}{2}}$ level. Were it not for uncertainty concerning this level, the $D_{\frac{5}{2}}$ phase shifts could be set approximately equal to the $D_{\frac{3}{2}}$ phase shifts.

Several measurements of σ_T have been made recently at this laboratory.[30,32,33] For a better comparison with the theory, these data are plotted in Fig. 5 in the form $k^2\sigma_T/4\pi$, together with a curve indicating the contribution of $D_{\frac{5}{2}}$ scattering if $\delta_2^+=\delta_2^-$. It will be noticed that while the total cross-section values for $E_n\geq 17$ Mev are accounted for by this assumption, the experimental points for E_n between 12 and 14 Mev fall even below the curve for $\delta_2^-=0$. Presumably these discrepancies are indicative of the unlocated $D_{\frac{5}{2}}$ resonance. Unfortunately, the angular distribution measurements at $E_n=14.3$ Mev could not be analyzed to give more information about the D interactions than is provided by the theory. Further high-energy total cross-section measurements are planned,[32] and analysis of the implications of p-He^4 scattering measurements at 31.6 Mev[34] is in progress.

[32] R. L. Henkel and J. E. Perry (private communication).
[33] R. B. Day and R. L. Henkel, Phys. Rev. **92**, 358 (1953).
[34] B. Cork, Phys. Rev. **89**, 78 (1953), and private communication to D. C. Dodder.

V. POLARIZATION AND SCATTERED NEUTRONS

Because of the strong spin-orbit forces involved, the n-He^4 interaction results in partial polarization of the scattered neutrons.[1,35–39] For an unpolarized incident beam of neutrons, the polarization of neutrons scattered through an angle θ in the center-of-mass system is directed along the normal to the plane of scattering. Its magnitude is given by[37]

$$P(\theta)=\langle\boldsymbol{\sigma}\rangle/\sigma(\theta)=(AB^*+BA^*)/(AA^*+BB^*), \quad (6)$$

where $\langle\boldsymbol{\sigma}\rangle$ is the expectation value for the spin in the normal direction, $\sigma(\theta)$ is the differential cross section, and A and B are the expressions within the absolute-square signs in Eq. (1), that is, $\sigma(\theta)=AA^*+BB^*$. Using Eq. (6), the polarization may be calculated for any angle and energy from the phase shifts given in Fig. 5. An example of the interesting possibility of using elastic scattering by He^4 as a polarizer or analyzer in experiments involving polarized neutrons has already been reported.[40] As an indication of the large degree of polarization available, $P(90°)$ has been calculated as a function of energy, and the results plotted in Fig. 6. Because of the uncertainties in the d-wave phase shifts, the curve is drawn only to 10 Mev, but the 90° polarization should remain roughly constant from 10 to 20 Mev, except in the vicinity of the $D_{\frac{5}{2}}$ resonance.

VI. CONCLUSION

The present experimental results for n-He^4 scattering are in substantial agreement with the predictions based on analysis of p-He^4 scattering experiments, and support equivalence of the mirror nuclei He^5 and Li^5.

The author wishes to thank Drs. J. H. Coon, E. R. Graves, and F. L. Ribe for their interest and assistance in the experimental details of this investigation, D. C. Dodder and J. L. Gammel for the results of their theoretical analysis, and J. H. Coon, J. E. Perry, R. B. Day, and R. L. Henkel for permission to quote the results of their total cross-section measurements in advance of publication.

[35] J. S. Schwinger, Phys. Rev. **69**, 681 (1946).
[36] L. Wolfenstein, Phys. Rev. **75**, 1664 (1949).
[37] J. V. Lepore, Phys. Rev. **79**, 137 (1950).
[38] R. J. Blin-Stoyle, Proc. Phys. Soc. (London) **A64**, 700 (1951).
[39] A. Simon and T. A. Welton, Phys. Rev. **90**, 1036 (1953).
[40] Bishop, Westhead, Preston, and Halban, Nature (London) **170**, 113 (1953).